Tutorial on Sampling-based POMDP-planning for Automated Driving

Henrik Bey[1][a], Maximilian Tratz[1], Moritz Sackmann[1][b], Alexander Lange[2] and Jörn Thielecke[1]

[1] *Institute of Information Technology, FAU Erlangen-Nürnberg, 91058 Erlangen, Germany*

[2] *Pre-development of Automated Driving, AUDI AG, 85045 Ingolstadt, Germany*

Keywords: Automated Driving, Decision Making under Uncertainty, POMDP.

Abstract: Behavior planning of automated vehicles entails many uncertainties. Partially Observable Markov Decision Processes (POMDP) are a mathematical framework suited for formulating the arising sequential decision problems. Solving POMDPs used to be intractable except for overly simplified examples, especially when execution time is of importance. Recent sampling-based solvers alleviated this problem by searching not for the exact but rather an approximated solution, and made POMDPs usable for many real-world applications. One of these algorithms is the Adaptive Belief Tree (ABT) algorithm which will be analyzed in this work. The scenario under consideration is an uncertain obstacle in the way of an automated vehicle. Following this example, the setup of POMDP and ABT is derived and the impact of important parameters is assessed in simulation. As such, this work provides a hands-on tutorial, giving insights and hints on how to overcome the pitfalls in using sampling-based POMDP solvers.

1 INTRODUCTION

In road traffic there are often situations whose future development cannot be predicted safely. These uncertainties arise due to an incomplete perception and limited predictability of other road users. Automation systems for the driving task are at least equally affected by these shortcomings compared to human drivers. On highways, for example, smaller obstacles such as potholes often cannot be safely recognized by vehicles' sensors until getting close. Further away, single detections are made, but these can also be interpreted as false positives. In this situation, the desired behavior would be a reduction of velocity which keeps the possibility for an emergency stop but does not react uncomfortably until the detection is certain.

The described scenario can be modeled as a POMDP—a mathematical framework for planning under uncertainty. Due to the nature of POMDPs, direct calculation of an optimal solution is not possible in limited time other than for extremely simple theoretical examples as they were shown to be PSPACE-complete (Papadimitriou and Tsitsiklis, 1987). For more difficult problems it is often desired to reach a *good enough* solution in finite time rather than spending much more time in search of the optimum. Such an approximated solution is provided by the new generation of online sampling-based POMDP solvers like the Adaptive Belief Tree (ABT) algorithm (Kurniawati and Yadav, 2016) examined in this work.

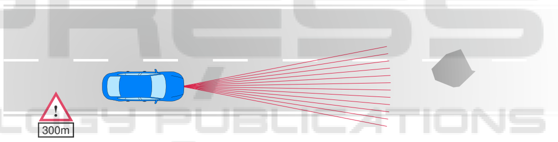

Figure 1: The automated vehicle approaches a potential obstacle. Its vision is impaired by fog. From the warning sign it knows about the obstacle, the question is whether it can be passed.

The key challenge in using ABT and other solvers is mapping the real-world problem to the abstract POMDP problem structure. Even if the real-world problem can rarely be chosen, it is crucial that its model is tailored to the algorithm. Otherwise it will work inefficiently or output no solution at all. The goal of this work is to develop an understanding of sampling-based POMDP solving in a way that allows for transfer to other problems.

A simple illustrative example of an automated vehicle approaching a potentially dangerous pothole in foggy weather (see Figure 1) will be introduced in Section 3. Following this example, the POMDP as a problem structure and its solution with the ABT will be explained. Moreover variations of important pa-

[a] https://orcid.org/0000-0003-4945-6802

[b] https://orcid.org/0000-0001-9341-5800

Bey, H., Tratz, M., Sackmann, M., Lange, A. and Thielecke, J.
Tutorial on Sampling-based POMDP-planning for Automated Driving.
DOI: 10.5220/0009344703120321
In *Proceedings of the 6th International Conference on Vehicle Technology and Intelligent Transport Systems (VEHITS 2020)*, pages 312-321
ISBN: 978-989-758-419-0

rameters will be analyzed. Thereafter, the problem will be extended by making the position of the obstacle variable (Section 4). Handling this additional dimension requires further considerations (Sunberg and Kochenderfer, 2018).

2 RELATED WORK

This work is based on the ABT algorithm (Kurniawati and Yadav, 2016) which is implemented in the "Toolkit for Approximating and Adapting POMDP Solutions in Real Time" (TAPIR) (Klimenko et al., 2014). ABT belongs to the new class of online sampling-based POMDP solvers. Its predecessor, "Partially Observable Monte-Carlo Planning" (POMCP) (Silver and Veness, 2010), and the "Determinized Sparse Partially Observable Tree" (DESPOT) (Somani et al., 2013; Ye et al., 2017) fall into the same category. They represent the *belief* (probability distribution over possible states) by a set of sampled states within a particle filter. The mapping of reachable beliefs to actions is calculated during runtime. On the contrary, offline solvers try to find the best action for *all* possible beliefs in advance. Staying with the example of automated driving, the latter can be dropped, because thinking of all possible traffic situations is infeasible. All three mentioned methods build a tree of sampled trajectories starting from the current belief. Also, they are *anytime-capable*, meaning that they improve the policy as long as they are given time. ABT differs from both other algorithms in that it is able to keep and only modify the tree if the model changes, whereas the others have to start from scratch. Also, in case of DESPOT, the tree is constructed in a different way.

This new generation of POMDP solvers recently found its way into the field of automated driving. For example, Hubmann et al. demonstrated in a series of publications how POMDP planning can be beneficial in different traffic scenarios. They applied the ABT algorithm to a crossroad scenario where the goal destination of other drivers is unknown to the agent (Hubmann et al., 2018a). Next, they looked at a merge scenario. This time, it was uncertain whether other drivers will cooperate and let the automated vehicle merge (Hubmann et al., 2018b). At last, potential objects in occluded areas are dealt with (Hubmann et al., 2019). Here, the existence of the occluded object is unknown. The same scenario was covered by Schörner et al. using ABT as well (Schörner et al., 2019). González et al. deal with a highway scenario, the uncertainty being the lane change intention of other traffic participants (González et al., 2019). They use a modified version of POMCP.

These five works choose the uncertainty to be a discrete variable representing either the other objects' destination, cooperation, existence or target lane. The reason being that this kind of solver is particularly suited for such problems as we will show later.

All of the aforementioned works focus either on a general explanation of the respective solver or on the application to a specific scenario. Instead, we want to explain the ABT solver following a comprehensible example and look in detail at solver-specific pitfalls in application and parameter variations.

3 SCENARIO: BINARY CASE

At this point we will introduce the scenario that is used to explain POMDPs as well as the mechanisms of the ABT solver.

The agent, an automated vehicle, starts at position $x_{\mathrm{v},0}$ with velocity $v_{\mathrm{v},0}$ and approaches a potential obstacle (e.g., pothole or lost truck tire), see Figure 1. It is equipped with a sensor (e.g., lidar) and knows about the obstacle's position x_{p} from external data (e.g., warning sign). But due to imperfect perception or adversarial weather conditions, its range of vision d_{view} is limited, thus it cannot recognize whether the obstacle is traversable (road blocked, obstacle exists $e_{\mathrm{p}} = 1$; or not, $e_{\mathrm{p}} = 0$) until getting closer. Ideally, the vehicle wants to pass the obstacle with its desired speed $v_{\mathrm{v},0}$ without braking, but on the other hand, crashing into the obstacle is unacceptable. The vehicle's actions are limited to deceleration/acceleration. The expected behavior is for the vehicle to slow down until it is certain about the obstacle's state and then to either stop or accelerate again. All parameters are summarized in Table 1 at the end of the next section.

The example is constructed to be as simple as possible while still retaining enough features to justify complex uncertainty planning. Both, the uncertain part of the state (road blocked or free) and the observation (obstacle recognized or not) can be described by binary variables which is why this scenario is called the Binary Case.

3.1 Partially Observable Markov Decision Process

POMDPs are a general mathematical framework allowing to describe various decision problems involving uncertainty. A POMDP is fully defined by the tuple

$$\langle S, A, O, T, Z, R, b_0, \gamma \rangle . \quad (1)$$

We will explain the POMDP by defining its eight components, taking the example from above. It is also these components that have to be implemented for the TAPIR/ABT.

States S: A state s describes all variable parts of the world relevant to the problem. In this special example only the vehicle's position x_v, its velocity v_v and the obstacle state e_p are relevant, thus $s = (x_v, v_v, e_p)^\mathsf{T}$. As x_v and v_v are continuous, the set of all possible states S is infinite.

Possible Actions A: The vehicle is limited to accelerations or decelerations. We allow for four different values: $A = \{-4\,\mathrm{m/s^2}, -2\,\mathrm{m/s^2}, 0\,\mathrm{m/s^2}, 2\,\mathrm{m/s^2}\}$.

Possible Observations O: The sensor may either recognize the obstacle ($o = 1$) or not ($o = 0$), so that $O = \{0,1\}$. Note that the lack of an obstacle detection might also be due to the limited range of vision, while due to sensor noise also false detections can be made.

Transition Function T: The transition function describes the probability of arriving in state s' after performing action (acceleration) a in state s: $T(s,a,s') = P(s'|s,a)$. For our example, we assume deterministic transitions. Typically, the time is discretized and we assume constant acceleration over one time step $\Delta t = 1\,\mathrm{s}$. The obstacle state remains constant.

$$\begin{bmatrix} x_v(t+\Delta t) \\ v_v(t+\Delta t) \\ e_p(t+\Delta t) \end{bmatrix} = \begin{bmatrix} 1 & \Delta t & 0 \\ 0 & 1 & 0 \\ 0 & 0 & 1 \end{bmatrix} \begin{bmatrix} x_v(t) \\ v_v(t) \\ e_p(t) \end{bmatrix} + \begin{bmatrix} \Delta t^2/2 \\ \Delta t \\ 0 \end{bmatrix} a(t) \tag{2}$$

Observation Function Z: Similarly, the observation function models the probability of receiving an observation o after performing action a and reaching state s': $Z(s',a,o) = P(o|s',a)$. This function is used to describe imperfect perception of the vehicle's sensors. For the sake of simplicity, we assume a simple, yet intuitive model that is only dependent on the distance $d = x_p - x_v$ to the potential obstacle position x_p. Very far away, the sensor always outputs zero, i.e., no obstacle detected. Getting closer increases the probability of a true positive measurement but also for false positives. Very close to the obstacle, it gets detected and correctly classified with high probability.

For the range $0 < d < d_{\mathrm{view}}$, the probabilities for true and false positives are given by

$$P(o=1|e_p=1) = \frac{1}{2} + \frac{1}{2}\cos\left(\frac{\pi\, d}{d_{\mathrm{view}}}\right) \tag{3}$$

$$P(o=1|e_p=0) = \frac{1}{2}\left(1 - \frac{d}{d_{\mathrm{view}}}\right)\sin\left(\frac{\pi\, d}{d_{\mathrm{view}}}\right) \tag{4}$$

Both curves are depicted in Figure 2. Outside the definition range (past the obstacle or beyond sensor range) the functions extend with a constant value of 0 or 1 respectively. As the observation is a binary variable, $P(o=0|e_p=1) = 1 - P(o=1|e_p=1)$ and $P(o=0|e_p=0) = 1 - P(o=1|e_p=0)$.

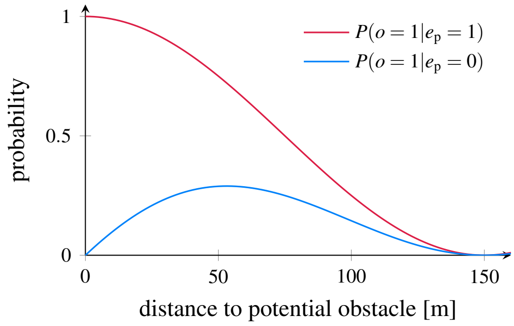

Figure 2: Probabilities of true positives (red) and false positives (blue) as a function of distance.

Reward Function R: The reward function $R(s,a)$ is the agent's moral compass, telling it what to do. We want the vehicle to keep its velocity and prevent braking, but foremost not to crash. Therefore, we award negative rewards for undesired events:

$$\begin{aligned} R(s,a) = w_{\mathrm{acc}} \cdot \sigma(-a)\, a^2 + w_{\mathrm{vel}} \cdot |v_{v,0} - v_v| \\ + w_{\mathrm{crash}} \cdot \sigma\left(x_v - x_p\right) \cdot e_p \end{aligned} \tag{5}$$

where $s = (x_v, v_v, e_p)$ and $\sigma(\diamond)$ denotes the Heaviside step function. The first term activates when braking, the last when crashed. Weights are needed to make the terms dimensionless and balance decelerations:

$$w_{\mathrm{acc}} = -4\,\mathrm{s^4/m^2}, \tag{6}$$

$$w_{\mathrm{vel}} = -1\,\mathrm{s/m}, \tag{7}$$

$$w_{\mathrm{crash}} = -10^6 \tag{8}$$

The rewards are constructed to be always negative, which proves useful later in Sec. 3.2.

Initial Belief b_0: In the beginning, our agent is certain about its position and velocity, but assumes a 50 % chance that the road is blocked ($b_0 = 0.5$). If more a priori information is available (e.g., about typical pothole occurrence rates) it can be included here.

Table 1: Parameters for the Binary Case.

Name	Symbol	Value	Unit
Existence obstacle (pothole)	e_p	$\{0,1\}$	-
Position obstacle	x_p	300	m
Initial position vehicle	$x_{v,0}$	0	m
Initial & target velocity	$v_{v,0}$	30	m/s
Range of vision	d_{view}	150	m
Time step	Δt	1	s
Initial belief obstacle state	b_0	0.5	-

Discount Factor γ: In our case, future rewards are not discounted, $\gamma = 1$. Lowering this factor may help if long-term predictions of the environment are difficult (e.g., when other traffic participants may enter the scene), as it decreases their impact on decision making.

3.2 Adaptive Belief Tree Algorithm

After defining the POMDP, we solve it with ABT (Kurniawati and Yadav, 2016) to find the (near) optimal *policy*. A policy maps beliefs to an action. In other words, the policy tells the agent what to do, depending on what it believes the state to be. Online sampling-based POMDP solvers derive the policy by building a tree of reachable beliefs, starting from the current belief. For illustration of the algorithm, a potential build-up of the belief tree is described in the following. To facilitate the explanation, the resulting tree is shown in Figure 3, with numbers added to the corresponding steps. The tree is simplified by depicting only two possible actions. The parameters used for ABT are listed in Table 2.

1. The algorithm starts with an initially empty tree by sampling one possible state (called a particle) from b_0 at ①. By chance, in the example, this particle has no obstacle (blue).

2. An action a is chosen randomly (here: acceleration) among the available actions. It is applied to the chosen particle's state which results in a new state according to the transition function T and yields an observation o by the observation function Z and a reward r defined by R. The particle lands in a new belief node ②. Both a and o are not real, they are a possible scenario which is "thought through" by the agent. Note that, while the action can be chosen actively, the received observation depends on T and Z, both of which may contain uncertainty. Thus, at this point the expansion of the tree cannot be controlled. As belief ② has not been visited before, exploration stops for this particle; the algorithm first wants to explore the breadth of the tree before going deep. To compensate for the truncated planning depth, a heuristic function may be called to estimate the remaining value of the belief that would result if it was further pursued. By default, the heuristic returns simply zero which fits to our reward function, designed to be always negative (or zero). Implicitly, this results in an optimistic estimate.

3. A second particle is sampled, for which an previously unperformed action is chosen. Obviously, also this particle ends in a new belief ③ after only one step. The trajectory of a particle, defined by its sequence of actions and observations, is called an *episode*.

4. After all available actions have been tried once, the main action selection mechanism of ABT comes into play, the Upper Confidence Bound for Trees (UCT) (Kocsis and Szepesvári, 2006). It balances the exploitation of known high-reward branches against the exploration of new or less visited parts of the tree. Each time, it chooses the action that maximizes a modified value estimate:

$$a_{\text{next}} = \arg\max_{a \in A} \left[\hat{Q}(b,a) + c_{\text{UCT}} \sqrt{\frac{\log |H_b|}{|H_{b,a}|}} \right], \quad (9)$$

where $\hat{Q}(b,a)$ is the estimated value of taking action a from belief b (the so-called Q-value-function). The second term adds a bonus to less explored actions depending on how many episodes take that action ($|H_{b,a}|$) compared to the total number of episodes running through that belief ($|H_b|$). The term is weighted by c_{UCT} which is an important parameter that controls exploration and will be investigated in Sec. 3.3.

The value $\hat{Q}(b,a)$ is estimated from previous episodes. By default, it is calculated as the average total reward of all episodes passing along a from the current level l down till the end of the episode $|h|$.

$$\hat{Q}_{\text{default}}(b,a) = \frac{1}{|H_{b,a}|} \sum_{h \in H_{b,a}} \left(\sum_{i=l}^{|h|} \gamma^{i-l} R(s_{h_i}, a_{h_i}) \right), \quad (10)$$

where $H_{b,a}$ denotes the episodes running through b and a, and $|\diamond|$ their count. s_{h_i} and a_{h_i} are state and action of episode h at layer i.

We found this to result in very conservative behavior, especially with highly negative rewards as for a crash. That is because the outer sum in (10) also includes episodes that act suboptimally (unnecessarily crash into the obstacle) since ABT tries all actions (step 2) when hitting a new belief. Therefore, we switched to the "max"-option implemented in TAPIR, being closer to 'taking action a and acting optimally thereafter' (Russell, 1998), which does not include suboptimal episodes:

$$\begin{aligned} \hat{Q}_{\max}(b,a) = & \frac{1}{|H_{b,a}|} \sum_{h \in H_{b,a}} R(s_{h_l}, a_{h_l}) + \\ & \gamma \sum_{o \in O} \frac{|H_{b,a,o}|}{|H_{b,a}|} \max_{a'} \left[\hat{Q}_{\max}(b'_{a,o}, a') \right]. \end{aligned} \quad (11)$$

$|H_{b,a,o}|$ is the number of episodes running through b, a and o. $b'_{a,o}$ denotes the belief (node) reached after performing a and receiving o; a' is the action in the next step. Although defined recursively, the value can easily be calculated within the tree in a bottom-up approach. As a drawback, this more optimistic estimate includes less episodes in its calculation and therefore may be less robust.

As our reward function disfavors braking, according to (9) the next action will be acceleration. Again,

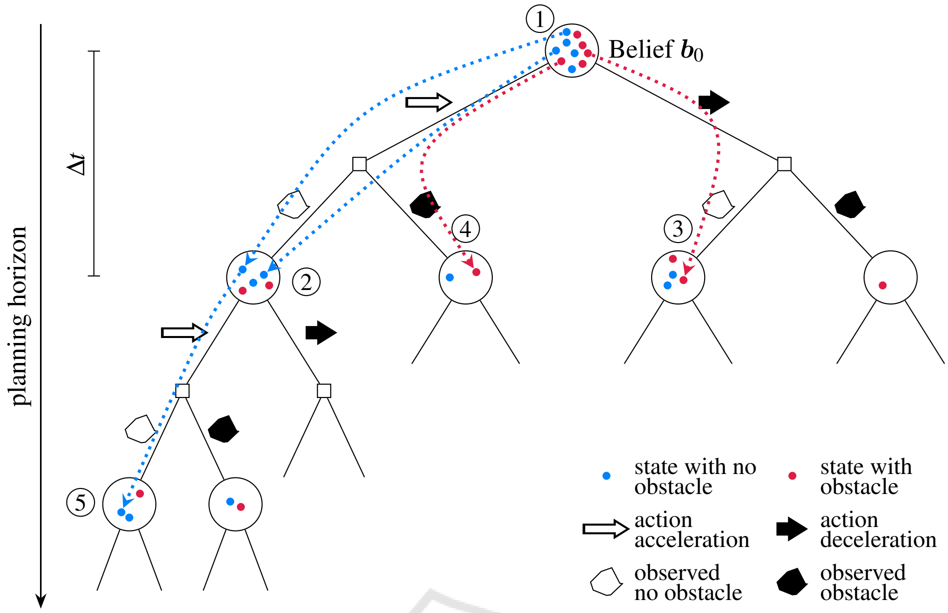

Figure 3: Simplified belief tree with several sampled episodes.

as observations cannot be controlled, the particle might receive another observation as in 2 and land in belief node 4 which terminates this episode.

5. Assuming a low c_{UCT}, the algorithm might choose to accelerate again for the fourth particle. Doing so, the particle might reach belief 2 which is not new this time. Thus, the episode is extended and a second action is selected and a new observation made, to end up for example at 4. After each episode, the values of the belief nodes are updated according to (11). By this, the new information is passed up the tree.

6. The procedure is repeated for a predefined number of episodes n_{epis} (here: 5000) or until a given time limit is reached. Running down deeper into the tree, eventually particles with a different obstacle state will be separated by observations and land in different belief nodes: A particle containing an obstacle is more likely to cause a positive observation and vice versa. This way, the POMDP factors in future information gain.

7. Now the agent has to decide for the real action. Instead of deciding after the UCT in (9) which rewards exploration, it chooses the action that maximizes the (approximated) Q-function $\hat{Q}(b,a)$ in (11), thus, exploiting the information in the tree. Afterwards, it receives an actual observation. In our case, it might decide to accelerate and see no obstacle. The corresponding belief at 2 is picked as the new root of the tree. All other branches of the former root can be pruned. The subtree under 2 is kept. Keeping parts of the tree between time steps is one of the key features of ABT, rendering it more efficient, as it does not have to start from scratch in each step. Ideally, the particles in the new root belief form a better representation of the actual state and the agent incrementally gets "smarter".

8. Like all particle filters, also ABT suffers from particle depletion. Particles explored with a different action at the first step or having received wrong observations are lost. Eventually, after several time steps no particle is left that fits the actual observation. To overcome this problem, ABT offers a default implementation to replenish particles. It tries to "force" particles from the previous belief into the new one by always choosing the action actually performed and "hoping" to receive the correct observation, until a minimum number of particles $n_{\text{min,part}} = 1000$ is reached at the new root. More efficient ways can be implemented by the user.

Table 2: Parameters ABT.

Name	Symbol	Value	Unit
UCT factor	c_{UCT}	1000	-
Episodes per step	n_{epis}	5000	-
Minimal particle count	$n_{\text{min,part}}$	1000	-
Maximum depth	-	20	-

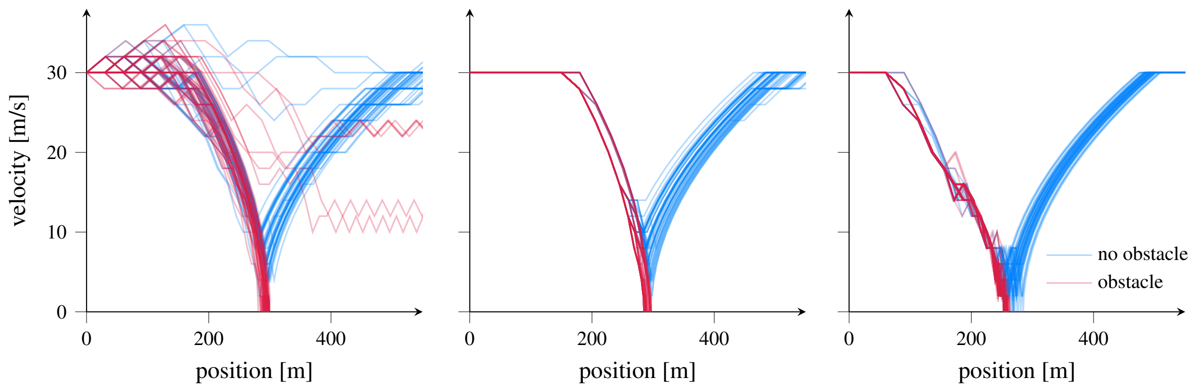

(a) $c_{\mathrm{UCT}} = 1,\ \hat{Q}_{\max}$ (b) $c_{\mathrm{UCT}} = 10^3,\ \hat{Q}_{\max}$ (c) $c_{\mathrm{UCT}} = 10^3,\ \hat{Q}_{\mathrm{default}}$

Figure 4: 50 simulated trajectories for each ABT configuration with and without obstacle.

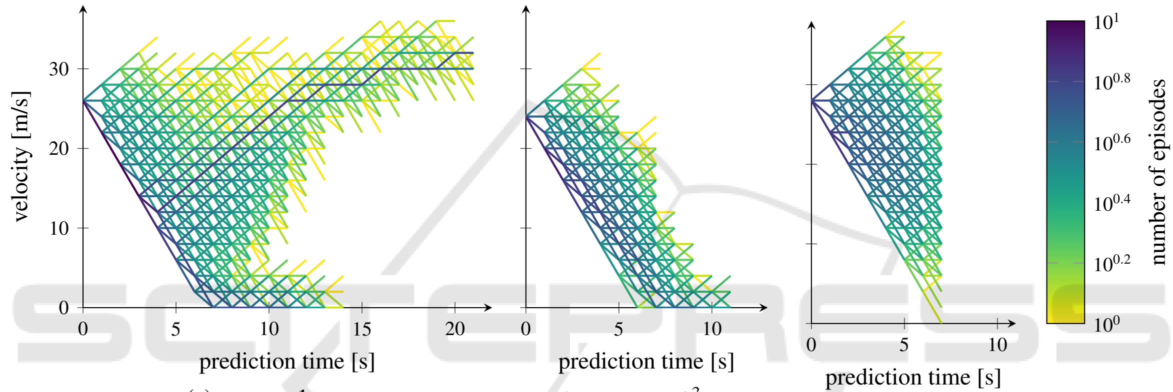

(a) $c_{\mathrm{UCT}} = 1$ (b) $c_{\mathrm{UCT}} = 10^3$ (c) $c_{\mathrm{UCT}} = 10^7$

Figure 5: Explored actions of 5000 episodes with no obstacle and different UCT-factors, sampled at $t = 7\,\mathrm{s}$ (simulation time). The color shows the number of episodes passing along the edge on a logarithmic scale. On the negative part of the prediction time, the trajectory taken so far is shown.

3.3 Analysis

The algorithm is analyzed in a small simulation environment of the above example. It uses the same models for state transition and observations as the POMDP model in Sec. 3.1. For real-life applications, this is a strong assumption and it would be safer to add artificial noise to both parts of the POMDP model to make ABT more robust. For our simulation, this is not needed.

Due to the probabilistic part of the observation function, both the “real” observations and the construction of the tree are non-deterministic. To enable a reliable evaluation, each parameter set was simulated 50 times. The resulting trajectories of three configurations are shown in Figure 4. The first, in Figure 4a, is an example for choosing c_{UCT} too low. The algorithm does not explore enough, subsequently in some cases it does not see the possibility of a crash and does not sufficiently reduce the velocity. In case of an obstacle (red) it then fails to stop in front of the obstacle at 300 m. After the crash, the reward function is dominated by the crash penalty so that the agent behaves irrationally.

Choosing an appropriate c_{UCT} results in a much more consistent behavior, as in Figure 4b. The agent shows the expected behavior, it slows down in front of the potential obstacle and once it is certain that there is no threat, it accelerates again. The point of accelerating again depends on the sequence of observations made. In Figure 4c the default Q-function from (10) with equal c_{UCT} is shown. Notice the more conservative behavior causing it to brake much earlier.

The effect of the UCT-factor can also be seen when looking at the belief tree; compare Figure 5a and Figure 5b. Both show the velocity curves of the sampled episodes in one planning step in one of the simulations. The exact tree highly depends on the observations made, therefore they are not directly comparable. Yet, it is obvious that a lower c_{UCT} leads to more selective

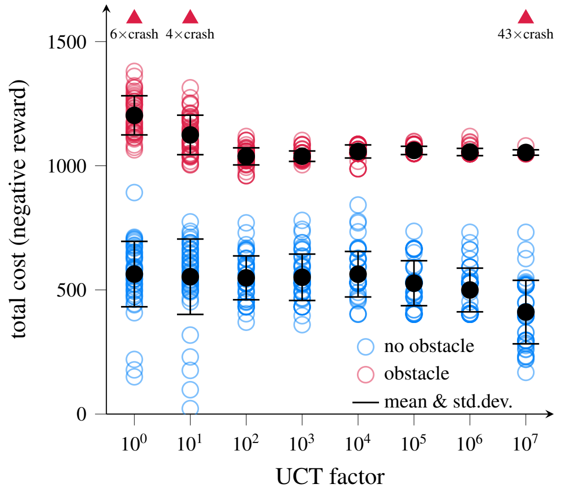

Figure 6: Total negative rewards of the simulations with mean and standard deviation. Crashes are excluded but shown at the top and lie in the range of 10^6.

exploration. The plan of slowing down for another 4 s and then speeding up again is clearly visible. On the plus side, the algorithm may focus on more promising regions of the tree. On the downside, it samples the edges less often and therefore might not encounter unlikely but disastrous observations.

This leads to another effect: A higher c_{UCT} leads to a shorter planning horizon. The reason being that, as all branches of the tree are explored more evenly, less episodes reach to a deeper level in the tree, as can be seen in Figure 5c. If the planning horizon falls below the time needed to make a stop, crashes cannot be prevented. Notice the higher velocity at the root node, indicating a more aggressive driving.

The final evaluation of the reached rewards with different UCT factors is shown in Figure 6. Due to the stochastic character of the observations both in building the tree and in the actual observations received, the results vary. Therefore, 50 Simulations were carried out with each configuration. The results confirm the deductions: A too low UCT-factor leads to too optimistic behavior, approaching the potential obstacle too fast and not being able to prevent crashes in all cases. Setting c_{UCT} too high, in turn, leads to a too short horizon and many crashes.

4 SCENARIO: CONTINUOUS CASE

The scenario from above is now extended in that the position of the potential obstacle is no longer known. The new scenario is depicted in Figure 7. The agent

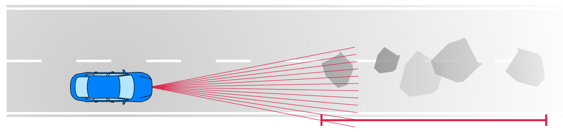

Figure 7: The position of the obstacle is no longer fixed but the agent expects it to lie in the marked area.

expects the obstacle to lie within a 2 km stretch starting at $x_{\text{p,start}}$. The obstacle is not guaranteed to exist. As in the Binary Case, there may be no obstacle at all. All other aspects of the scenario are left untouched: Except for the obstacle position, all parameters from Table 1 are still valid. Within the simulation, the obstacle is always placed at the same position (if existing) without loss of generality. The new parameters are listed in Table 3.

Table 3: Parameters for the Continuous Case.

Name	Symbol	Value	Unit
Obstacle zone start	$x_{\text{p,start}}$	300	m
Obstacle zone end	$x_{\text{p,end}}$	2300	m
Actual position	x_{p}	500 or $\emptyset$	m

4.1 Model Changes

The new scenario has to be represented by changes in the model. In the following, the affected components of the POMDP as in (1) are mentioned.

States S: In addition to the vehicle states and the obstacle existence, the new state also encompasses the obstacle position x_{p} as a hidden variable: $s = (x_{\text{v}}, v_{\text{v}}, e_{\text{p}}, x_{\text{p}})^{\mathsf{T}}$. While the vehicle states have been continuous already, the new state variable also renders the unobservable part continuous, adding complexity to the problem.

Possible Observations O: When close enough, the agent may perceive the distance d_{meas} to the obstacle and can deduce its position. Therefore, observations now consist of two components: $o' = (o, d_{\text{meas}})^{\mathsf{T}}$ with the observed existence $o \in \{0, 1\}$ already introduced.

Observation Function Z: The probability functions for observing the obstacle existence $P(o|e_{\text{p}})$ remain unchanged as in (3) and (4). Note that this still allows for false positives. Additionally, the distance measurements have to be included. For sake of simplicity, we assume that the distance is correctly measured if a positive existence measurement is received. Otherwise, the laser hits nothing and d_{meas} is simply set to the range of vision d_{view}.

$$d_{\text{meas}} = \begin{cases} x_{\text{p}} - x_{\text{v}} & \text{for } o = 1, \\ d_{\text{view}} & \text{else .} \end{cases} \tag{12}$$

Initial Belief b_0: As in the previous case, the agent has to make assumptions about the hidden states before the start. We stick to the 50 % chance that there is an obstacle at all. For the obstacle position, it is assumed to lie within the interval from $x_{\mathrm{p,start}}$ to $x_{\mathrm{p,end}}$. That means that the obstacle positions for the particles in b_0 are drawn from an uniform distribution. By default, particles are drawn using a random generator. Here, we enforced an actually uniform distribution by evenly placing the obstacles over the interval, which slightly increases the reproducibility. The initial distribution can also be seen in Figure 8.

4.2 Complications in Solving

The continuous observations and continuous hidden states pose problems for the ABT algorithm. We will analyze those problems looking at Figure 8. On the left at 0 s the uniform distribution of the particles can be seen. Note that only those particles are shown that contain an obstacle ($e_{\mathrm{p}} = 1$). As all particles are freshly sampled, they are highlighted in red. At this point the agent (blue) is still far away, its field of vision does not reach the potential obstacle positions, yet. Therefore, the agent gained no information.

4.2.1 Particle Depletion

Still, because ABT only keeps those particles that took the same action and received the same observation, inherently, particles get lost, because they were not

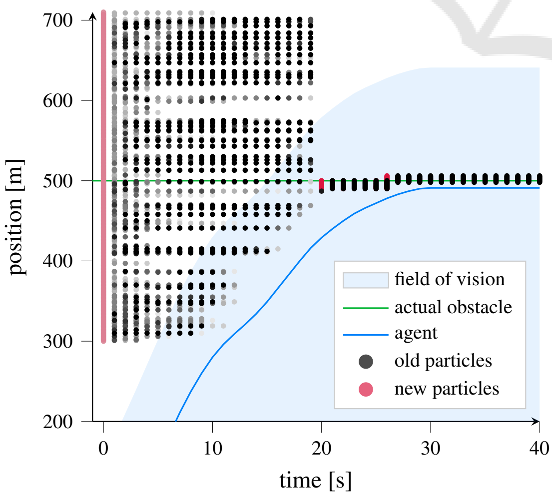

Figure 8: The potential obstacle positions in the particle filter are shown over the course of a simulation. For reference, also the agent, its field of view and the actual obstacle position are shown. When the agent gets closer to the particle positions, negative observations make their existence less likely. When the agent receives the first positive measurement at 20 s, it is able to brake in time. $c_{\mathrm{UCT}} = 10^3$.

'lucky' enough to land in the right belief. This equals a loss of information. The so-called particle depletion is a common problem for particle filters but especially severe with the ABT and continuous states. The reason being, that the ABT does not perform regular resampling as it tries to keep the subtree, while moving or generating new particles would mean to loose their episodes. This behavior is opposed to the DESPOT solver which uses an independent conventional particle filtering algorithm including importance resampling (Thrun et al., 2005).

This problem aggravates with increasing domain size. The larger the state space, the more particles are required for an adequate representation. Especially further dimensions (e.g., a moving obstacle) or infinite domains (obstacle position not restricted) will lead to failure without special consideration.

The effect of particle depletion can be seen at 20 s in Figure 8 when the agent receives its first positive measurement. At this point hardly any particles are close to the observed position. Therefore, emergency resampling is started, which creates particles close to the observed location. Obviously that is very inefficient as the tree has to be re-calculated almost from scratch.

4.2.2 Infinite Branching Factor

Another problem arises from the continuous observations. All three algorithms, ABT, POMCP and DESPOT, were designed for discrete observations (and actions). Whenever a new observation is made, a new observation branch and subsequent belief are opened up. In case of continuous observation this would mean that each particle lands in its own belief, degenerating the tree just after one step. There are methods to counteract this issue, one of them being *progressive widening* (Couëtoux et al., 2011) which artificially limits the number of available observations at each action node, forcing episodes to run deeper into the tree. Progressive widening and its drawbacks are analyzed in (Sunberg and Kochenderfer, 2018).

Another option, that may also be activated in ABT, is to use discretization. Here, two observations are considered equal if a certain distance function falls below a preset threshold. In that case, the episode is routed into the same belief. If the considered particle may not be assigned to any existing belief, a new belief node is set up. If several beliefs are possible, the episodes pick the closest belief according to the distance function.

One possible distance function uses the observed existence and distance:

$$\Delta(o_i,o_j) = \begin{cases} 0 & \text{if } o_i = 0 \wedge o_j = 0, \\ |d_{\text{meas},i} - d_{\text{meas},j}| & \text{if } o_i = 1 \wedge o_j = 1, \\ \infty & \text{else} \end{cases} \quad (13)$$

When both observations are negative, they are considered equal. If both are positive, the observations are as far apart as the observed distances. If the existence observations differ, they must not be equal. The equality is determined by

$$\Delta(o_i,o_j) \leq \Delta_{\max}\,. \quad (14)$$

Now, the threshold $\Delta_{\max}$ plays an important role, in addition to the UCT-factor in the Binary Case. The results of different parameter choices are shown in Figure 9. Two effects can be seen: When the maximum distance is chosen small, the algorithm can precisely react to the observation, resulting in general in lower costs. On the other hand, a low maximum distance leads to narrow and therefore many belief nodes, corresponding with a fine-grained but not deep search tree. In the extreme case at $\Delta_{\max} = 1\,\text{m}$, the horizon is too short, such that braking in time is not always possible.

On the other end, greater distances allow for less observation branches and deeper trees, but they face another problem: If a belief stretches over a large section, there may be trajectories passing through that belief and not crashing, even though the obstacle lies within that section. The reason being, that the obstacle is simply ‘further behind’ within the section spanned by the belief. In such a case, the belief may receive a good value estimate, making it attractive, even though it is dangerous. The resolution is simply too coarse.

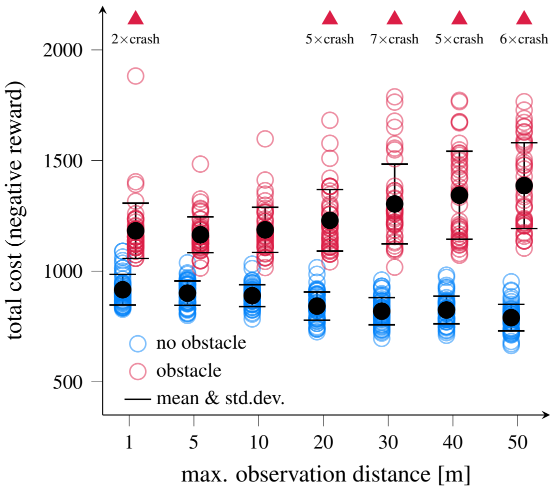

Figure 9: Total negative rewards of the simulations with different maximum observation distances. Crashes are again shown at the top. Each configuration was simulated 50 times. $c_{\text{UCT}} = 10^3$.

4.2.3 Short Horizon

Hand in hand with the above issue goes the problem of a too short horizon. As there are more possible observations, the branching factor is increased, the tree gets wider and shallower. With $n_{\text{epis}} = 5000$ episodes, the algorithm only reaches a planning horizon of 6-7 steps. As already shown in Figure 5c and Figure 6, that is not enough to prevent crashes. And indeed, the algorithm crashes often when used in this configuration. For that reason we make use of the heuristic already mentioned in Step 2 in Section 3.2. The heuristic is called when an episode hits a new belief node. It returns a first estimate for the value of the belief. As a heuristic we use the Intelligent Driver Model (IDM) (Treiber and Kesting, 2013) in a discretized version (accelerations are rounded to the available actions in A, see Section 3.1). The situation in the particle (including hidden states) is simulated forward until the planning horizon (20 steps) using the accelerations of the IDM as actions for the agent. This helps to detect beliefs that inevitably crash into the obstacle and should be avoided; the horizon is artificially prolonged.

Using the heuristic and choosing UCT-factor and maximum observation distance wisely leads to a reasonable behavior as in Figure 10. Before the agent enters the potential obstacle zone starting at 300 m, it has already reduced its velocity. When the obstacle appears at $x_{\text{p}} = 500\,\text{m}$, the agent is slow enough to prevent a crash in all cases. When there is no obstacle, the agent continues with lowered speed until the danger zone is left.

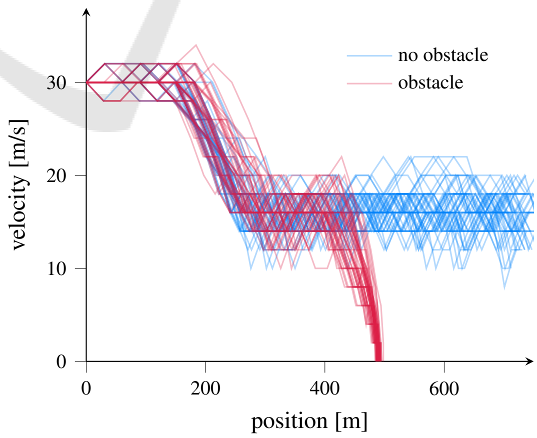

Figure 10: Simulated trajectories with the obstacle position unknown to the agent. 50 runs each for no obstacle and obstacle at $x_{\text{p}} = 500\,\text{m}$. The potential obstacle zone starts at $x_{\text{p,start}} = 300\,\text{m}$. As the agent reduces its velocity sufficiently in advance, it never crashes. The fluctuation in velocity is due to under-sampling. There are not enough episodes to reproduce the fine difference in the cost function.

5 CONCLUSION & OUTLOOK

In this work we presented the scenario of an uncertain obstacle in automated driving. The example was used to motivate and explain the use of POMDPs. We derived its components and explained the functionality of the ABT solver. Even though the chosen scenario was kept simple, it is complex enough to point out five different difficulties that have to be overcome when trying to solve a real world problem. At the simpler scenario with a fixed obstacle position, we demonstrated the impact of the UCT-factor, balancing exploration versus exploitation, and suggested using a suitable estimate for the Q-value-function. Extending the scenario to include continuous hidden states and observations brought further problems. Namely, we could show the need for discretizing observations in order to prevent a degenerated tree, and pointed at the influence of the particle filter. Lastly, the advantage of using a heuristic function as a first estimate for a belief value was explained.

Even though we did not solve a burning problem in this work, we hope to pave the way for others into POMDP-based behavior planning by bringing insights into the mechanisms. Especially at the advent of parallelizing solver algorithms (Cai et al., 2018), promising to alleviate the massive drawback of the computational burden, we expect to find POMDPs in more and more applications. Apart from speeding up the algorithms, we see need for further research in handling continuous observations. Perhaps, smart discretization combined with progressive widening may help in that regard.

ACKNOWLEDGMENT

This research was supported by AUDI AG.

REFERENCES

Cai, P., Luo, Y., Hsu, D., and Lee, W. S. (2018). Hyp-despot: A hybrid parallel algorithm for online planning under uncertainty.

Couëtoux, A., Hoock, J.-B., Sokolovska, N., Teytaud, O., and Bonnard, N. (2011). Continuous upper confidence trees. In *International Conference on Learning and Intelligent Optimization*, pages 433–445. Springer.

González, D. S., Garzón, M., Dibangoye, J., and Laugier, C. (2019). Human-like decision-making for automated driving in highways. In *2019 IEEE 22nd International Conference on Intelligent Transportation Systems (ITSC)*.

Hubmann, C., Quetschlich, N., Schulz, J., Bernhard, J., Althoff, D., and Stiller, C. (2019). A pomdp maneuver planner for occlusions in urban scenarios. In *2019 IEEE Intelligent Vehicles Symposium (IV)*, pages 2172–2179.

Hubmann, C., Schulz, J., Becker, M., Althoff, D., and Stiller, C. (2018a). Automated driving in uncertain environments: Planning with interaction and uncertain maneuver prediction. *IEEE Transactions on Intelligent Vehicles*, 3(1):5–17.

Hubmann, C., Schulz, J., Xu, G., Althoff, D., and Stiller, C. (2018b). A belief state planner for interactive merge maneuvers in congested traffic. In *2018 IEEE 21st International Conference on Intelligent Transportation Systems (ITSC)*, pages 1617–1624.

Klimenko, D., Song, J., and Kurniawati, H. (2014). Tapir: A software toolkit for approximating and adapting pomdp solutions online. In *Proceedings of the Australasian Conference on Robotics and Automation, Melbourne, Australia*, volume 24.

Kocsis, L. and Szepesvári, C. (2006). Bandit based monte-carlo planning. In *European conference on machine learning*, pages 282–293.

Kurniawati, H. and Yadav, V. (2016). An online pomdp solver for uncertainty planning in dynamic environment. In *Robotics Research*, pages 611–629. Springer.

Papadimitriou, C. H. and Tsitsiklis, J. N. (1987). The complexity of markov decision processes. *Mathematics of operations research*, 12(3):441–450.

Russell, S. J. (1998). Learning agents for uncertain environments. In *COLT*, volume 98, pages 101–103.

Schörner, P., Töttel, L., Doll, J., and Zöllner, J. M. (2019). Predictive trajectory planning in situations with hidden road users using partially observable markov decision processes. In *2019 IEEE Intelligent Vehicles Symposium (IV)*, pages 2299–2306.

Silver, D. and Veness, J. (2010). Monte-carlo planning in large pomdps. In *Advances in neural information processing systems (NIPS)*, pages 2164–2172.

Somani, A., Ye, N., Hsu, D., and Lee, W. S. (2013). Despot: Online pomdp planning with regularization. In *Advances in neural information processing systems (NIPS)*, pages 1772–1780.

Sunberg, Z. N. and Kochenderfer, M. J. (2018). Online algorithms for pomdps with continuous state, action, and observation spaces. In *Twenty-Eighth International Conference on Automated Planning and Scheduling*.

Thrun, S., Burgard, W., and Fox, D. (2005). *Probabilistic robotics*. MIT press.

Treiber, M. and Kesting, A. (2013). *Traffic Flow Dynamics: Data, Models and Simulation*. Springer.

Ye, N., Somani, A., Hsu, D., and Lee, W. S. (2017). Despot: Online pomdp planning with regularization. *Journal of Artificial Intelligence Research*, 58:231–266.